High power DPSS laser micro-machining of stainless steel and silicon for device singulation

D. Karnakis, G. Rutterford, M. R. H. Knowles

Oxford Lasers Ltd., Unit 8, Moorbrook Park, Didcot, Oxfordshire OX11 7HP, UK

Abstract

We describe high power diode-pumped solid-state (DPSS) laser micro-machining results of commonly used industrial materials such as stainless steel and silicon. Frequency up-converted lasers were used at 532nm and 355nm. We discuss the benefits of high laser intensity (~ GW/cm^2) micro-machining for efficient laser micro-fabrication. At such high irradiance conditions material properties are approaching their critical limits and ablation mechanisms are complex. These can be exploited to our advantage in particular for micro-drilling and micro-cutting small feature sizes in the order 10-20 μm and high aspect ratios of up to 20:1. Etch rate data are presented and a comparative study of the ablation efficiency in these materials is discussed. Results of single shot and multiple shot ablation are also presented. The potential applications of this technology to device singulation for electronic and power generation devices will be described.

Keywords: laser, micro-machining, steel, silicon, ablation

1. Introduction

During the last decade the increasing demand for miniaturisation of micro-system devices and their associated components has established laser micro-machining as the preferred fabrication method in many industrial sectors [1]. Laser micro-drilling and micro-cutting of common industrial materials has been investigated by many academic and industrial teams with emphasis mainly on attaining suitable quality while maximizing processing speed [2]. The continuing reduction in the desirable feature size has consequently increased the overall aspect ratio and therefore 2.5D laser micro-machining is used in most cases. Besides the high average laser power, which facilitates a financially viable process, high laser intensity is necessary as well to overcome processing limitations that commonly arise from the high aspect ratio micro-fabrication. Diode-pumped solid-state (DPSS) lasers offer high power and high laser intensity in the visible and UV. We will show that these lasers can present unique advantages for processing silicon, and stainless steel when optimized at very high irradiance.

2. Experimental setup

The aim of this study was to investigate the laser ablation characteristics of silicon and stainless steel under high intensity, nanosecond duration exposure as a method to optimize device singulation. Samples of crystalline silicon and stainless steel were cleaned in alcohol prior to laser irradiation. Their thickness varied between 0.275-1.5mm. Two laser wavelengths were used, 532 and 355 nm. All the lasers exhibited near diffraction limited intensity profiles and were focussed on the target surface using plano-convex lenses of focal length f=50mm (355nm) and f=100mm (532nm). The lasers could be practically operated between 1Hz-100kHz and an x-y table carrying the samples was synchronized to the laser frequency to generate the desirable features. The incident laser power was varied using a half waveplate and polarization cube in the beam path. A laser trepanning head was inserted prior to the objective lens to rotate the laser beam accordingly. A galvanometer scanner (20mm aperture) was also used for the high speed percussion drilling of stainless steel, equipped with a telecentric lens of focal length f=100mm. The surface morphology of the resulting features was investigated by scanning electron microscope and with an optical microscope with ±1 μm spatial resolution. Additionally a negative impression of single-shot craters in silicon was created using a vinyl polysiloxane paste and then analyzed using the microscopes. All experiments were conducted in atmospheric pressure in air.

Table 1. Summary of main laser characteristics

Laser	Nd:YAG	Nd:YVO_4
λ (nm)	355	532
P_{max} (W)	5	11
E_p (mJ)	0.5	0.22
PRF (kHz)	10	50
τ (ns)	45	13
M^2	<1.3	<1.3

3. Results and Discussion

3.1. Laser processing of silicon (355nm)

A tightly focused UV DPSS laser (355nm) with a Gaussian intensity spatial profile enables high laser intensity on target and thus higher material removal rates. Silicon micromachining applications such as wafer dicing for IC packaging, channel scribing or hole drilling for microfluidic device fabrication, benefit in particular from such an approach. An optical trepanning device was used and this combined with high laser intensity enables laser drilling of high aspect ratio micro-holes in silicon.

In figure 1, laser drilled holes are shown in a 375μm thick silicon wafer using a 355nm Nd:YAG. Rapid material removal was accompanied by a remarkably good edge quality with very little collateral damage around the hole rim and excellent hole roundness that compare well with ultra-fast laser machining of silicon. A thin sacrificial layer covering the wafer surface was used prior to laser exposure, which was removed immediately afterwards. Surface contamination, consisting mainly of undesirable silicon micro-particles and redeposited molten material, that usually accompanies laser micro-machining of silicon could thus be avoided.

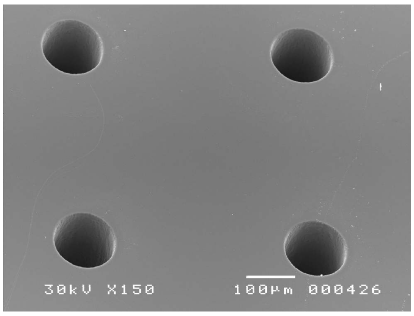

Fig.1 Laser trepanned holes in silicon using high intensity (15 GW/cm^2) at 355nm.

A single-shot laser ablation study of silicon using high laser intensities was also undertaken in order to examine the material response and optimise further laser micromachining. Negative imprints of the resulting craters were created (Figure 2) and subsequently analysed. The imprints illustrate that the craters do not exhibit a uniform spatial profile. The crater diameter is quite large near the surface of incidence but narrows significantly approaching the laser spot size dimensions with increasing depth. The shape of the crater can be best described by a one-sheeted semi-hyperboloid.

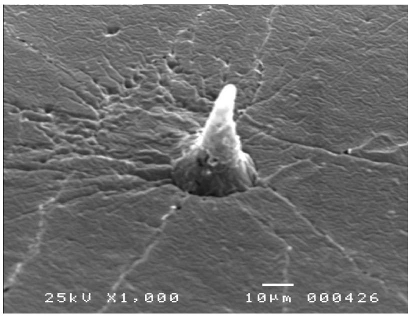

Fig.2 SEM of a negative imprint of a single-shot laser ablation crater in silicon using 355nm at 19 GW/cm^2 .

Figure 3 shows the single-shot etch depth measurements and calculated ablated crater as a function of laser irradiance using a 355nm DPSS laser with pulse width of 45ns (FWHM). The optical microscope measurements shown here were also verified using the dental paste negative imprints of the inspected craters. The ablated volume was estimated using equation 1

$$V = \pi h(2a^2 + R^2)/6 \qquad (1)$$

where a is the crater radius at the crater floor, R the crater surface radius and h the crater depth.

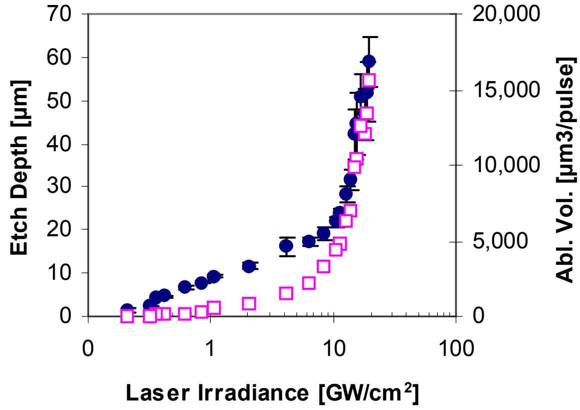

Fig.3 Single-shot etch depth (solid circle) and ablated crater volume (open square) measurements of crystalline silicon as a function of incident laser irradiance at 355nm.

The measured depth grows steadily with increasing laser intensity reaching a value of almost 22 µm at about 10.5 GW/cm^2. This ablation rate is generally considered quite high for silicon at 355 nm. But an even steeper rise in etch depth is observed with increasing the incident laser intensity further beyond 10 GW/cm^2, eventually reaching a value of 58µm at 19 GW/cm^2. A single-shot ablation threshold of 0.16 GW/cm^2 can be deduced from this data, assuming a Beer's law relation between the etch depth and laser irradiance, which corresponds to a laser fluence threshold of 7.1 J/cm^2.

Such high etch depth values in silicon have not been reported before using ns lasers. The ablation depth per pulse is typically close to the optical absorption length or thermal diffusion length near the ablation threshold. Here the absorption depth of a^{-1} ~ 10nm is almost three orders of magnitude lower although the thermal diffusion depth $\chi_D=(4D\tau)^{½}$ of 4µm is low but comparable to the observed etch depths near threshold. This suggests that a thermally driven ablation mechanism is more likely involved which varies considerably within the intensity range considered.

Rapid heating rates exceeding 10^{12} K/sec at these laser intensities could raise the surface temperature of silicon near the critical limit almost instantly and give rise to dramatic density fluctuations. An explosive boiling mechanism could provide a plausible explanation for the large amounts of material expelled from the crater. Similarly high etch rates up to 20µm per pulse at 22 GW/cm^2 have been reported before for single-shot ablation of silicon at 266nm and have been attributed to a homogeneous bubble nucleation phase explosion ablation mechanism [5].

The ablated volume of the crater shows a similar behaviour to the etch depth curve. The volume increases gradually with laser intensity but a steep increase is observed beyond 10 GW/cm^2 reaching values of 1.5×10^4 µm^3 at 19 GW/cm^2. The surface crater diameter used in the volume calculation is seen to increase linearly with the logarithm of laser intensity. From a laser micro-machining viewpoint, it is useful to know the average volume of material removed per input unit energy. These data are shown on Figure 4, where the ratio of the ablated volume per incident pulse energy is plotted as a function of incident laser irradiance. The results indicate that the amount of material removed per unit input energy increases linearly with the logarithm of laser irradiance between 0.1-1 GW/cm^2. A drop is observed though for higher irradiance values between 1-10 GW/cm^2, which suggests that the ablation mechanism has changed in that region and becoming energetically more expensive. Namely, a volume of 41 μm^3 can be ablated using 1 μJ at intensity 1 GW/cm^2 but only 29 μm^3 can be removed using 1 μJ at the higher irradiance value of 6.3 GW/cm^2. For even greater laser intensities, the V/E_p ratio increases rapidly again reaching almost 68 μm^3/μJ for the highest irradiance value examined here. A commonly reported etch rate saturation effect that deviates from linear character of laser ablation could be related to our observations. It is typically attributed to the attenuation of incoming laser light from emerging ablation products that tend to absorb and/or scatter the incident laser beam above the irradiated crater resulting in less overall energy deposited in the material surface.

If we define ablation efficiency, n, (equation 2), in terms of the ratio of energy required to evaporate unit volume to the energy required to ablate unit volume,

$$n = \rho C(T_b - T_0)V/E_p \quad (2)$$

where ρ=2.3 g/cm^3 is the density, C=0.711 J/g K the specific heat capacity at room temperature T_0 and T_b=3151 K the vaporisation temperature of silicon, we can plot the ablation efficiency against incident laser irradiance (Figure 4). Notably only a fraction of the input energy is used to raise the temperature to the vaporisation point with the majority of the energy being used to remove the ablated material from the surface.

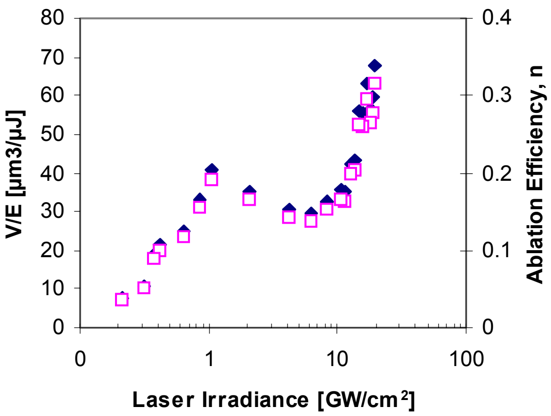

Fig.4 Ablation volume per unit input energy (V/E_p) (solid diamonds) and ablation efficiency (open square) as a function of incident laser irradiance at 355nm.

At very high laser intensity the ablation efficiency is highest, which is contrary to the established view that laser ablation is more efficient near the ablation threshold. It should be noted that the laser-induced plasma above the surface could contribute towards heating the surface and prolonging laser ablation when becoming very hot. In that sense the ablation efficiency is enhanced at high laser intensity by a combined laser and plasma etching process.

3.2 Laser drilling of stainless steel (532 nm)

High speed laser drilling of stainless steel is of interest for applications that require large numbers of micro-holes such as chemical filters, catalysts, membranes and medical devices. Stainless steel is a robust, rigid and inert material that is suitable for use in many chemical, medical and high temperature environments. In most applications the number of holes is in the range of 10,000 to 1,000,000 with a density of typically 100 – 600 holes per square millimetre in plate thicknesses of 0.05 – 0.4mm. The hole diameter is typically 5-25μm and the drilling speed must be higher than 100 holes per sec to make the application economically attractive.

Percussion drilling using high intensity on the target surface of the order 10 GW/cm^2 was used with a spot size of approximately 15 μm in diameter. This ensured that small diameter holes could be drilled with the minimum number of laser pulses possible. By varying the laser intensity appropriately, the hole size could be varied with good resolution enabling hole diameters as low as 3 μm which is smaller than the theoretical laser spot size. At such high intensities, a volume boiling mechanism drives laser ablation and so collateral damage and large heat affected zones are expected. In this case post processing may be necessary and chemical cleaning removes all loosely attached debris. The benefits of high-speed laser drilling and flexibility for rapid prototyping can offset any quality or additional manufacturing step issues.

By measuring the number of laser pulses required to penetrate the stainless steel plate, the average etch depth per pulse can be plotted against incident laser irradiance (Figure 5). At the highest available pulse energy, the laser intensity is so high, that only 30 laser pulses are required to drill through, averaging an etch rate of 10 μm/pulse and enabling a drill rate of over 200 holes per second. These remarkably high etch rates have only been reported before in laser ablation studies where superheating driven phase explosion phenomena are involved near the critical temperature of materials as mentioned above. It should also been pointed out that during high aspect ratio drilling the initial laser pulses remove on average more material than the final ones which are attenuated due to the long plume of ablated material trying to emerge from the bottom of the narrow cavity. So the ablation depth per pulse is expected to be a lot higher for the initial laser shots in this experiment.

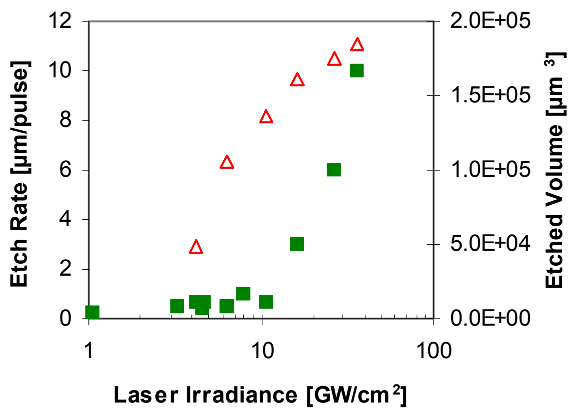

Fig.5 Average etch rate (solid square) and ablated volume (open triangle) in stainless steel as a function of incident laser irradiance at 532nm.

The ablation efficiency for stainless steel, as defined by Eq.2, is also plotted in Figure 6 as a function of incident laser irradiance. We used ρ=7.7 g/cm^3 for density, C=0.45 J/g K for specific heat capacity (at T_0) and T_b=3293 K for the vaporisation point of stainless steel. A very similar behaviour pattern to the previously mentioned silicon emerges in this case as well, even though a different laser wavelength was used. Less than 2% of the input energy is used to raise the temperature near the vaporisation point for the irradiance range between 1-10 GW/cm^2. But for higher irradiation levels above 10 GW/cm^2 the drilling efficiency increases rapidly reaching values of 8% for 36 GW/cm^2. Similarly the ablation efficiency is maximised for high laser intensity and not near the ablation threshold as customary believed.

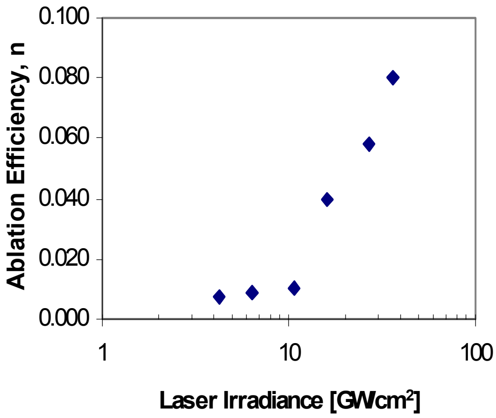

Fig.6 Ablation efficiency of stainless steel as a function of incident laser irradiance at 532nm.

The emergence of the hydrodynamic plume of ablated products above the target or within the high aspect ratio cavity must play a major role in this observation. Plasma enhanced etching has been previously reported [6] for high intensity laser ablation of metals. It is believed that the expanding ablation plume above the irradiated target becomes gradually ionised by absorbing an increasingly larger fraction of the incoming laser beam and this results in hotter plasma. The hot plasma re-radiates heat towards the ablated surface, thereby prolonging the heating period and resulting in a higher etch rate. Laser ablation efficiency refers therefore to a combined laser and plasma enhanced etching process efficiency as described for silicon above.

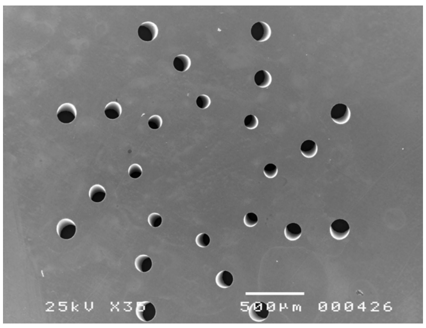

Fig.7 High aspect ratio laser drilling of a stainless steel fuel-injection nozzle.

High intensity laser drilling of stainless steel is also used in fuel-injection nozzle manufacturing. Figure 7 shows a certain configuration gasoline injection nozzle having three different diameter holes drilled at various angles to the surface normal. An auto trepanning head equipped with an optical taper correction module was used to enhance drilling speed and provide accurate control on the hole eccentricity. No gas assist was used.

4. Conclusions

We have investigated high laser intensity ablation of silicon and stainless steel using single-shot and multiple shot etch depth measurements. We have demonstrated that high quality efficient laser micro-machining can be accomplished using high laser intensity from diode-pumped solid state lasers at 532 and 355 nm comparable to ultrafast laser machining. The key to this process is the combined application of high peak and average power on target. We have determined that the ablation efficiency in air for stainless steel and silicon, although initially fluctuating, is greater towards higher intensities beyond a certain threshold, contrary to the established view that laser ablation is more efficient near the ablation threshold. A combined laser and plasma enhanced etching process could be responsible for such behaviour. Also it was shown that 355 nm single-shot laser ablation efficiency in silicon is almost an order of magnitude higher near threshold compared to visible 532 nm laser ablation of metals. At high intensities we have demonstrated single shot ablation depths of nearly 60 microns in silicon.

Acknowledgements

We gratefully acknowledge the support of Lightwave Electronics Corporation and Spectra-Physics GmbH for the loan of the lasers used in this study.

References

[1] Dunsky, D. (2005) Laser material processing in microelectronics manufacturing: status and near-term opportunities in Proceedings SPIE Conference on Laser Applications in microelectronic and Optoelectronic Manufacturing X, San Jose, California, USA, Vol.5713, 200-214

[2] Karnakis, D.M., Rutterford, G. & Knowles, M.R.H. (2005) High power DPSS laser micro-machining of silicon and stainless steel in Proceedings of the Third international WLT Conference on Lasers in Manufacturing, Munich, Germany, 741-746

[3] Föhl, C.; Dausinger, F. (2003) High precision deep drilling with ultrashort pulses. In Proceedings SPIE 4th International Symposium on Laser Precision Microfabrication, Munich, Germany, Vol.5063, 346-351

[4] www.mathworld.wolfram.com

[5] Yoo, JH., Jeong, SH., Mao, XL., Greif, R., Russo, RE. (2000) Evidence for phase-explosion and generation of large particles during high power nanosecond laser ablation of silicon, Applied Physics Letters, Vol. 76, No.6, 783-785

[6] Boley C.D., Early J.T., (1994) Proc. Laser Material Processing Conf, ICALEO'94, Orlando, FL, 79, 499